Integrator Sensitivity of Chaos in the Ultradian Glucose-Insulin Model

Aitijhya Sinha*, *Sourav* Chowdhury, and *Suparna* Roychowdhury

Postgraduate and Research Department of Physics, St. Xavier's College (Autonomous), Kolkata, India

Abstract. Diabetes mellitus is a long-term metabolic disorder. It happens when the glucose–insulin system does not work properly. As a result, blood glucose levels are not well controlled. The ultradian model helps describe the main processes of this system. It includes nonlinear interactions, time delays, and feedback effects. Because of this, the model can represent both normal and diseased conditions. In this paper, the dynamical behavior of the glucose-insulin regulatory system is studied, incorporating periodic pulsatile forcing. We investigate the system using a range of numerical integrators and employ multiple chaotic indicators, including the Maximal Lyapunov Exponent and Fast Lyapunov Indicator, over a large number of kick-relaxation cycles to characterize its dynamical nature. Our results reveal that the choice of integrator and its computational efficiency play a crucial role in the observed behavior and the values of these chaotic indicators. Based on these non-trivial findings, we present a detailed initial analysis of this newly identified integrator-sensitive behavior, quantifying the performance and sensitivity of different integrators with respect to multiple chaotic indicators. This analysis will help us to understand the dynamics of the glucose-insulin regulatory system at a deeper level and thus enable the suggestion of possible cures for this widespread disease.

1 Introduction

Diabetes mellitus is a chronic metabolic disorder in which blood glucose levels remain consistently high. This usually happens because of problems in insulin secretion, insulin action, or sometimes both. In simple terms, the condition develops when insulin-the main hormone responsible for regulating blood glucose-is either not produced in enough quantity or is not properly used by the body's tissues. As a result, glucose starts to accumulate in the bloodstream beyond normal levels [1]. Therefore, understanding glucose-insulin regulation is very important, as it provides insight into the underlying physiological behavior of diabetes mellitus.

Research on glucose-insulin regulation has improved understanding of disease progression and treatment, leading to several mathematical models [2, 3]. The ultradian model is particularly important, linking physiological processes with nonlinear dynamics [4-6]. In the Sturis *et al.* model [5], glucose stimulates insulin secretion, but its action is

*Corresponding author: sinhaaitijhya00@gmail.com

delayed affecting glucose uptake and production [7]. This delay is modeled using "remote insulin" compartments representing slower intracellular processes [8]. When we consider the combined effects of nonlinear insulin secretion, nonlinear hepatic glucose output, and this delayed insulin action, the system is able to generate self-sustained oscillations on its own, even without any external input [9]. Overall, the ultradian model shows how delays, nonlinearities, and feedback interactions come together to produce realistic oscillatory behavior in endocrine systems. Karamched *et al.* [10, 11], whose work is the primary inspiration behind this paper, have developed an ODE-based model that includes a linear delay filter and also incorporates an external nutritional input (periodic pulsatile kick). Their work refined the earlier works done by Sturis *et al.* [5], Drozdov *et al.* [4], and many others [6].

In this paper, we have used the model proposed by Karamched *et al.* and its parameters to study the glucose dynamics [11]. We investigate the system using a range of numerical integrators and employ multiple chaotic indicators, including the Maximal Lyapunov Exponent (MLE) and Fast Lyapunov Indicator (FLI), over a large number of kick-relaxation cycles to characterize its dynamical nature. Our results reveal that the choice of integrator and its computational efficiency play crucial roles in the observed behavior and the values of these chaotic indicators. We find that these chaotic transitions are highly sensitive to the integration scheme and can be significantly altered or even suppressed depending on the numerical method employed. We present a detailed initial analysis of this newly identified integrator-dependent behavior, quantify the performance and sensitivity of different integrators with respect to the chaotic indicators, and provide a direct comparison with earlier published results.

2 The Ultradian Model for Glucose-Insulin Regulation

The ultradian model is a key framework in theoretical and computational endocrinology, describing the nonlinear, delayed feedback between glucose and insulin that produces natural oscillations. Proposed by Sturis *et al.* [5], it includes two main negative feedback loops: insulin suppresses glucose production, and glucose stimulates insulin secretion. The model is formulated as a compartmental system with three state variables-plasma insulin (I_p), interstitial insulin (I_i), and plasma glucose (G). These variables are dynamically coupled through a three-stage linear delay filter that approximates the physiological delay between insulin secretion, transport, and its action on glucose production. Hence, the model produces a six-dimensional phase space. Since the delay is a three-stage linear filter, the system is finite-dimensional. This ultradian model was subsequently modified by Karamched *et al.* (referred to as the U-K model), where they introduced a conceptually different modification, not to the intrinsic physiology of the model but to its external driving mechanism [10, 11]. Karamched *et al.* replaced this input with instantaneous glucose impulses, mathematically represented as Dirac-delta "kicks" instead of continuous meal absorption. These impulses produce discrete jumps in the glucose state of the system, transforming the continuous time delay-driven ODE model into a hybrid dynamical system consisting of smooth evolution punctuated by discrete state resets. A schematic block diagram of this U-K model representing the glucose-insulin dynamic system, inspired by Karamched *et al*., is shown in Fig. 1 [11].

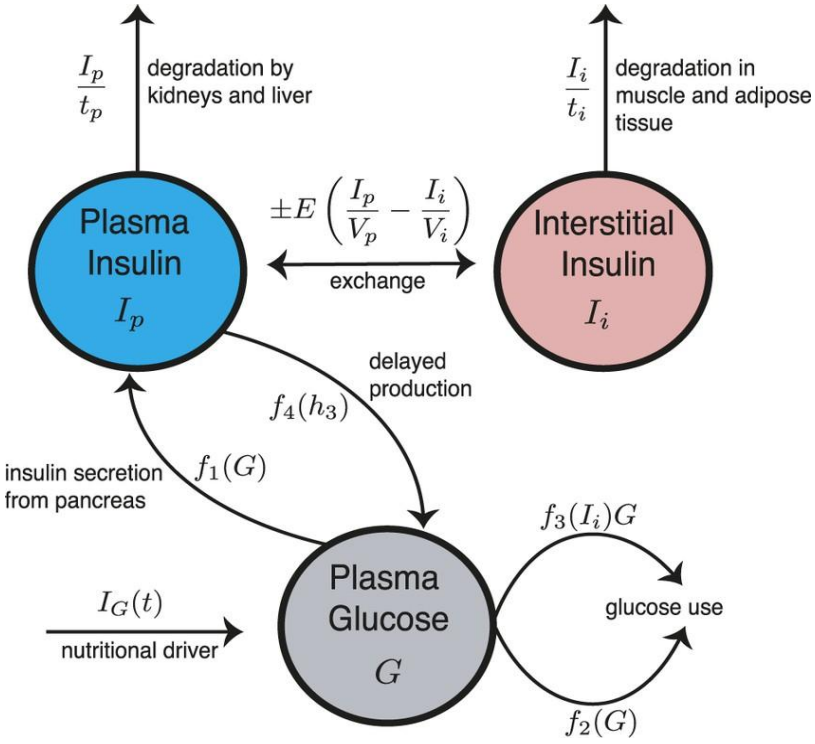

Fig. 1. block diagram of the ultradian model [11].

The equations representing this U-K model [11] are given below:

$$\frac{dI_p}{dt} = f_1(G) - E\left(\frac{I_p}{V_p} - \frac{I_i}{V_i}\right) - \frac{I_p}{t_p} \quad (1a)$$

$$\frac{dI_i}{dt} = E\left(\frac{I_p}{V_p} - \frac{I_i}{V_i}\right) - \frac{I_i}{t_i} \quad (1b)$$

$$\frac{dG}{dt} = f_4(h_3) + I_G(t) - f_2(G) - f_3(I_i)G \quad (1c)$$

$$\frac{dh_1}{dt} = \frac{1}{t_d}(I_p - h_1) \quad (1d)$$

$$\frac{dh_2}{dt} = \frac{1}{t_d}(h_1 - h_2) \quad (1e)$$

$$\frac{dh_3}{dt} = \frac{1}{t_d}(h_2 - h_3), \quad (1f)$$

where $f_1(G)$ represents the glucose-dependent insulin secretion, $f_2(G)$ represents insulin-independent glucose utilization, $f_3(I_i)G$ represents insulin-dependent glucose utilization, $f_4(h_3)$ represents insulin-dependent hepatic glucose release, $I_G(t)$ represents the external nutritional drive, $E(I_p/V_p - I_i/V_i)$ represents exchange between interstitial and plasma insulin, $I_p/t_p, I_i/t_i$ represents plasma and interstitial insulin degradation, respectively and h_1, h_2, h_3 represents delay process between plasma insulin and glucose production. The functional forms of these are

$$f_1(G) = \frac{R_m}{1 + \exp\left(-\frac{G}{V_g C_1} + a_1\right)} \tag{2a}$$

$$f_2(G) = U_b\left(1 - \exp\left(-\frac{G}{C_2 V_g}\right)\right) \tag{2b}$$

$$f_3(I_i) = \frac{1}{C_3 V_g}\left(U_0 + \frac{U_m - U_0}{1 + (\kappa I_i)^{-\beta}}\right) \tag{2c}$$

$$f_4(h_3) = \frac{R_g}{1 + \exp\left(\alpha\left(\frac{h_3}{C_5 V_p} - 1\right)\right)}, \tag{2d}$$

with

$$\kappa = \frac{1}{C_4}\left(\frac{1}{V_i} - \frac{1}{E t_i}\right) \tag{3}$$

The description of model parameter and their default values are given in Table 1 [11, 12].

2.1 Dynamical Analysis of the Intrinsic System

An intrinsic system refers to a dynamical model whose evolution is governed solely by its internal mechanisms, without dependence on external forcing or exogenous inputs. In this type of systems, the model equations fully encode all feedback loops, regulatory interactions, and nonlinear couplings that determine the state trajectories.

In the intrinsic system, where external nutritional input is absent ($I_G(t) = 0$; refer to Eq. (1c)), the qualitative behavior is governed entirely by the interaction among nonlinear components and the inherent time scales of the system [10]. The model self-organizes its dynamics, generating self-sustained oscillations or more complex fluctuations solely through its internal feedback mechanisms. Since, external forcing is absent, all dynamical transitions such as quasi-periodicity or chaotic behavior arise directly from parameter-driven bifurcations within the system. Thus, the study of this intrinsic system is important to understand the dynamical organization of the model without any external influences.

In the intrinsic U-K model, the parameter t_d controls the timing properties of the delayed insulin feedback that regulates hepatic glucose production. Instead of acting as a discrete time lag, t_d appears through a three-stage linear filter that converts plasma insulin I_p into the effective delayed signal h_3. Each stage in this cascade is characterized by the same time constant t_d, so increasing its value uniformly slows down the propagation of information through the filter [11]. This modification affects the system's linear stability. For small t_d,

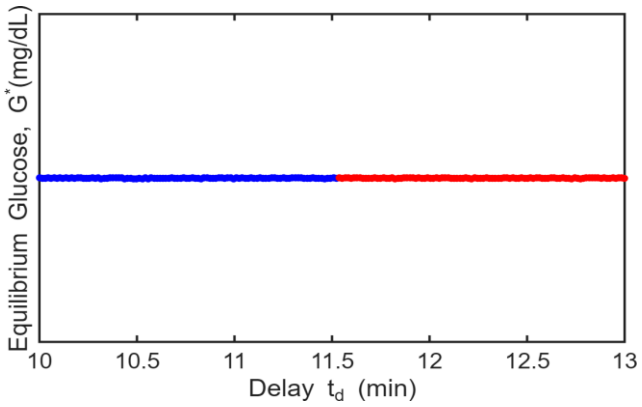

Fig. 2. The bifurcation diagram of glucose equilibrium points with respect to the delay t_d (the U-K model). The stable and unstable equilibrium points represent as blue and red, respectively.

Table 1. Description and the default values of parameters for the U-K model. IIGU: insulin-independent glucose utilization, IDGU: insulin-dependent glucose utilization, GDIS: glucose-dependent insulin secretion, and HGP: hepatic glucose production [11,12].

Name	Nominal value	Meaning
V_p	3 L	volume of plasma
V_i	11 L	volume of interstitial space
V_g	10 L	volume of glucose space
E	0.2 L min^{-1}	exchange rate for insulin between interstitial and plasma compartments
t_p	6 min	time constant for plasma insulin degradation
t_i	100 min	time constant for interstitial insulin degradation
t_d	10.5 min	delay between plasma insulin and hepatic glucose production
R_m	209 mU min^{-1}	maximal pancreatic insulin secretion rate
a_1	6.6	exponential constant affecting insulin secretion
C_1	300 mg L^{-1}	exponential scaling constant affecting GDIS
C_2	144 mg L^{-1}	exponential scaling constant affecting IIGU
C_3	100 mg L^{-1}	scaling constant affecting IDGU
C_4	80 mU L^{-1}	insulin sensitivity scaling factor affecting IDGU
C_5	26 mU L^{-1}	exponential scaling constant affecting HGP
U_b	72 mg min^{-1}	maximal rate of IIGU
U_0	4 mg min^{-1}	basal rate of IDGU
U_m	94 mg min^{-1}	maximal rate of IDGU
R_g	180 mg min^{-1}	maximal hepatic glucose production rate
α	7.5	exponential constant affecting HGP
β	1.772	hill coefficient affecting IDGU

rapid feedback stabilizes the system near equilibrium. As t_d increases, slower feedback allows oscillations to develop. When $t_d > t_d^*$, the eigenvalues which is a pair of complex conjugate crosses the imaginary axis, occurring supercritical Hopf bifurcation (Fig. 2) [10, 11, 13], which destabilizes the fixed point and produces a self-sustained limit cycle (Fig. 4). The critical value t_d^* is approximately 11.4 min marks the transition from steady state to sustained oscillations [10]. Initially, the system settles into a stable equilibrium, but once the time delay exceeds the critical value t_d^*, oscillatory behavior emerges (Fig. 3). Beyond this threshold, a stable limit cycle is born in this system, which corresponds to persistent glycemic oscillations (Fig. 4).

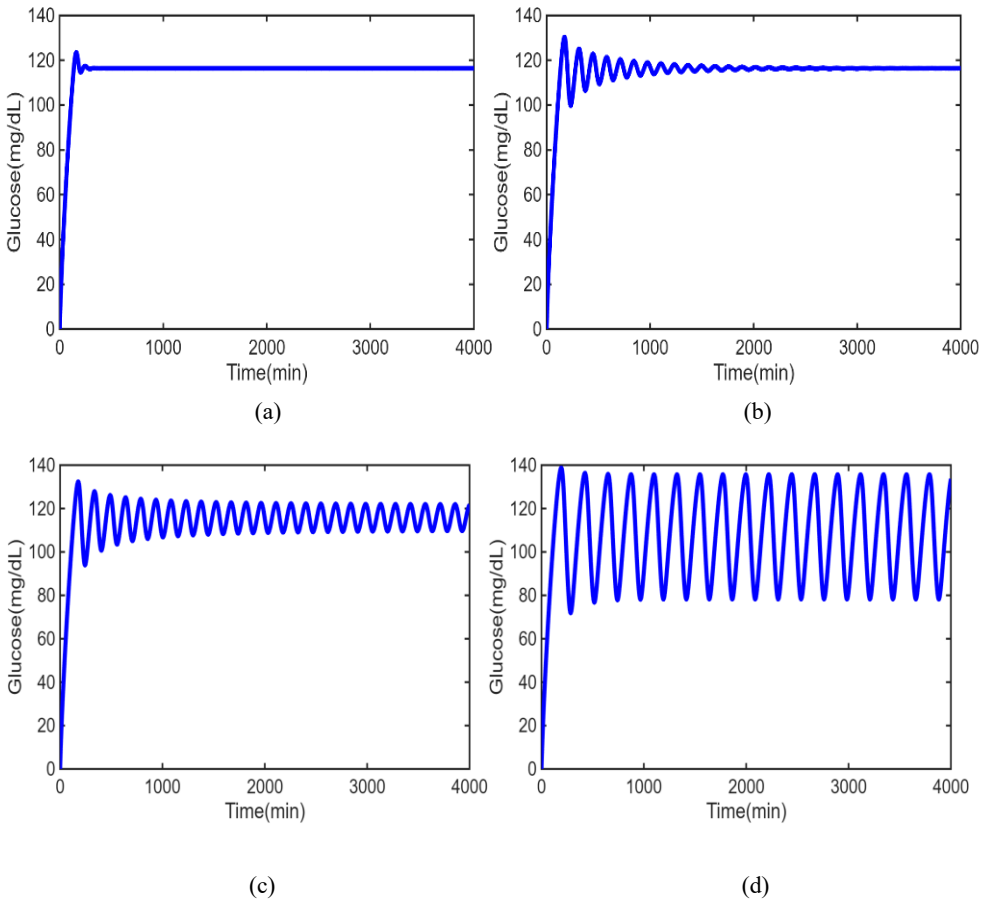

Fig. 3. The time series plot of glucose dynamics for the intrinsic U-K model when (a) t_d = 4 min, (b) t_d = 10 min, (c) t_d = 12 min and (d) t_d = 20 min.

2.2 Dynamical Analysis for Periodic Pulsatile Forcing

The term $I_G(t)$ in the U-K model (Eq. (1c)) represents the external nutritional drive (meal ingestion). The meal ingestion is given by

$$I_G(t) = \sum_{n=1}^{\infty} A_n \, \delta(t - T_n) \tag{4}$$

where $\delta(t)$ is the Dirac delta distribution (unit impulse), T_n is the time of meal n, A_n is the quantity of carbohydrate in meal n. This external nutritional input, $I_G(t)$, acts as a pulsatile kick. Between two consecutive kicks ($T_{n-1} < t < T_n$), the system evolves like an intrinsic system, i.e. Eq. (1) with $I_G(t) = 0$. At time T_n of meal n, the plasma glucose variable G is modified to $G + A_n$. At that time, T_n, the intrinsic system is paused, and the diffeomorphism is applied to the phase space [11].

$$(I_p, I_i, G, h_1, h_2, h_3) \mapsto (I_p, I_i, G + A_n, h_1, h_2, h_3)$$

For simplicity, considering only periodic pulsing ($T_n = nT$), where $T \in \mathrm{R}_{>0}$ is the inter-kick time) with constant kick amplitude ($A_n = A$ for all $n \in \mathrm{Z}_{\geq 0}$). Then Eq. (4) is now

$$I_G(t) = A \sum_{n=1}^{\infty} \delta(t - nT) \tag{5}$$

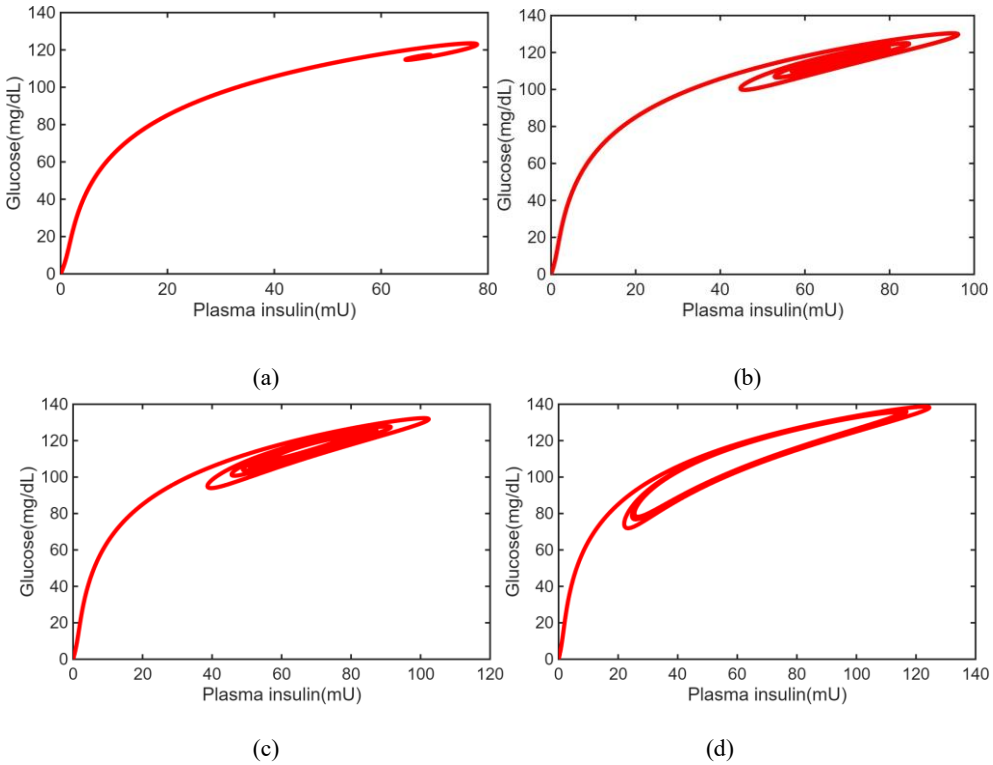

Fig. 4. The projection of phase space trajectory of glucose-plasma insulin space for the intrinsic U-K model when (a) t_d = 4 min, (b) t_d = 10 min, (c) t_d = 12 min and (d) t_d = 20 min.

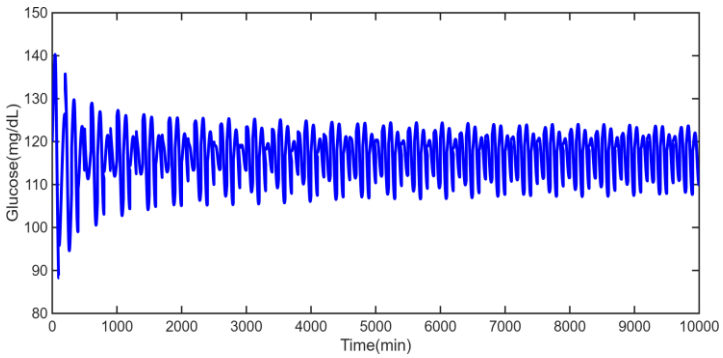

Fig. 5. The time series of glucose dynamics for the U-K model with T-periodic pulsatile forcing (Eq. (5)). Forcing parameters: A = 10 mg/dL, T = 100 min.

In Fig. 6, the phase space trajectory for the U-K model densely fills a bounded region without forming a strange attractor, suggesting quasi-periodic motion on a torus. This behavior is consistent with that observed in periodically forced nonlinear oscillators, where paths stay confined but do not close and indicates non-chaotic behavior. The response in Fig. 5 shows a typical periodically forced nonlinear oscillator, where internal oscillations combine with external forcing to produce smooth amplitude and phase modulation, rather than chaos. This behavior usually indicates quasi-periodic dynamics unless strong nonlinear resonance occurs.

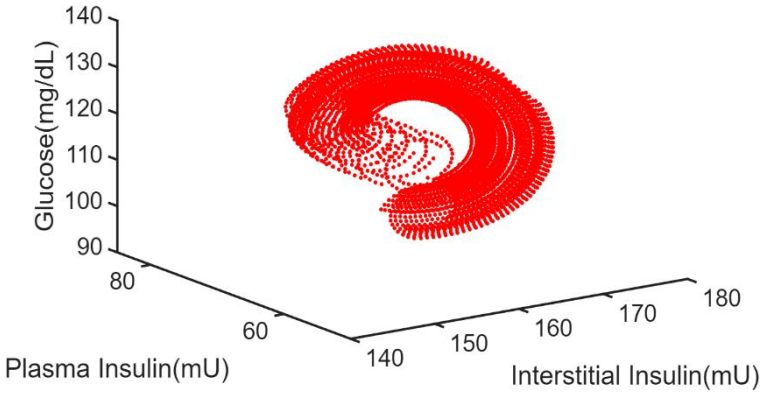

Fig. 6. The phase space for the U-K model with T-periodic pulsatile forcing (Eq. (5)). Forcing parameters: A = 10 mg/dL, T = 100 min. Such a structure is consistent with quasi-periodic motion on an invariant torus, as observed in forced nonlinear oscillators.

3 Integrator Sensitivity in Nonlinear Systems

In nonlinear systems, the choice of numerical integrator plays a significant role in determining the observed dynamics. This sensitivity becomes evident when different solvers produce different trajectories for the same problem. In many cases, this is not due to the system itself, but rather due to how the numerical method handles local errors. [14]. This sensitivity appears when we get different trajectories using different numerical solvers, even when the same differential equations and initial conditions are used. Intrinsic nonlinear features such as strong coupling, discontinuities, stiffness, and sensitivity to initial conditions can amplify small numerical errors and distort long-term behavior. Explicit methods may introduce artificial damping or excess energy, while implicit methods can smooth out important variations, making results solver-dependent. This effect is more pronounced in chaotic systems, where errors grow exponentially, so even small differences in methods can produce entirely different trajectories.

Tolerance settings have a strong effect on results, since adaptive integrators choose step sizes based on method-dependent error estimates. Changes in these tolerances can build up over time and affect how well the numerical solution matches the true dynamics [15], leading to different results for different solvers, especially in systems with discontinuities, delays, or strong nonlinearities. Since using very small tolerances is often not practical, the observed behavior may depend on the solver.

In biological systems (e.g., glucose–insulin, epidemiological, and ecological models) [16], even small numerical errors can change oscillation amplitudes and misrepresent the system's behavior. For chaotic systems, long-time statistical properties may differ across integrators unless carefully designed schemes are used. Hence, the accuracy of numerical

simulations of any system is highly dependent on the choice of integrator, as numerical errors can be exponentially magnified over time, potentially leading to qualitatively incorrect results.

4 Quantification of Chaos: Lyapunov Characteristics

Lyapunov characteristics quantify the sensitivity of a dynamical system to small perturbations by examining how infinitesimally close trajectories diverge or converge over time. The measure is the Lyapunov exponent, which gives the average exponential rate of separation: positive values indicate chaos, zero denotes periodic or quasi-periodic motion, and negative values denote stable dynamics. Because Lyapunov exponents require long integration times to converge, several fast indicators have been developed. In Fast Lyapunov Indicator (FLI), the deviation vector typically grows exponentially due to strong local instability, resulting in the FLI increasing very sharply with time for a chaotic system and for a periodic or quasi-periodic system, it grows slowly. Smaller Alignment Index (SALI), Generalized Alignment Index (GALI) are also there to quantify chaos. Together, the Lyapunov exponents, FLI, SALI, and GALI form a set of powerful tools for identifying and characterizing chaotic behavior in nonlinear dynamical systems [17]. In this paper, we have studied only MLE and FLI for the given system (refer to Eq. (1)).

4.1 Maximal Lyapunov Exponent (MLE)

In the existing literature, a variety of chaos indicators have been proposed [17]. In this work, we employ the Lyapunov exponent, since it is straightforward to implement and can reliably discriminate between ordered and chaotic behavior in our system, and remains effective across a wide range of dynamical parameters. The Lyapunov exponent measures the exponential divergence of two neighboring trajectories that start from infinitesimally close initial conditions. In a phase space of n dimensions, there are n such exponents, corresponding to each principal direction of growth or contraction. In the long-time limit ($t \to \infty$), the largest of these exponents dominates the divergence behavior; this is referred to as the maximal Lyapunov exponent (MLE).

We compute the maximal Lyapunov exponent (MLE) as follows. Two solutions of the system (refer to Eq. (1)) are integrated simultaneously, starting from initial conditions separated by $d_0=10^{-8}$. One solution is treated as the reference (or base) orbit, while the second is represented as a perturbation. Between successive kicks, (T_{n-1}, T_n), the unforced differential equations are integrated using MATLAB's ode45 integrator with default tolerances, and transient trajectories are discarded to ensure that only the steady-state dynamics are analyzed. After each kick-relaxation cycle, we compute the instantaneous separation d_k before the integration scheme is the same as the previous (d_k/d_0) in a vector [11]. The perturbed orbit is then renormalized by rescaling it so that its separation from the base orbit is reset to d_0. This procedure is repeated for $N=10^5$ kick-relaxation cycles, yielding a vector of N values of $\ln(d_k/d_0)$ [11]. The average of this vector provides the estimate of Λ_{max}, which quantifies the mean exponential divergence (or expansion rate) per kick-relaxation cycle:

$$\Lambda_{\max} = \frac{1}{N}\sum_{k=1}^{N} \ln\left(\frac{d_k}{d_0}\right),$$

where d_0 is the fixed initial separation, d_k is the separation after the k-th kick-relaxation cycle, and N is the total number of cycles. In the limit $N \to \infty$, Λ_{max} gives the average exponential

divergence per cycle. Fig. 7 shows that the maximal Lyapunov exponent remains negative or lie very close to zero for all parameter values, confirming that trajectories do not diverge exponentially. In a forced oscillatory system, this indicates periodic or quasi-periodic behavior rather than chaos.

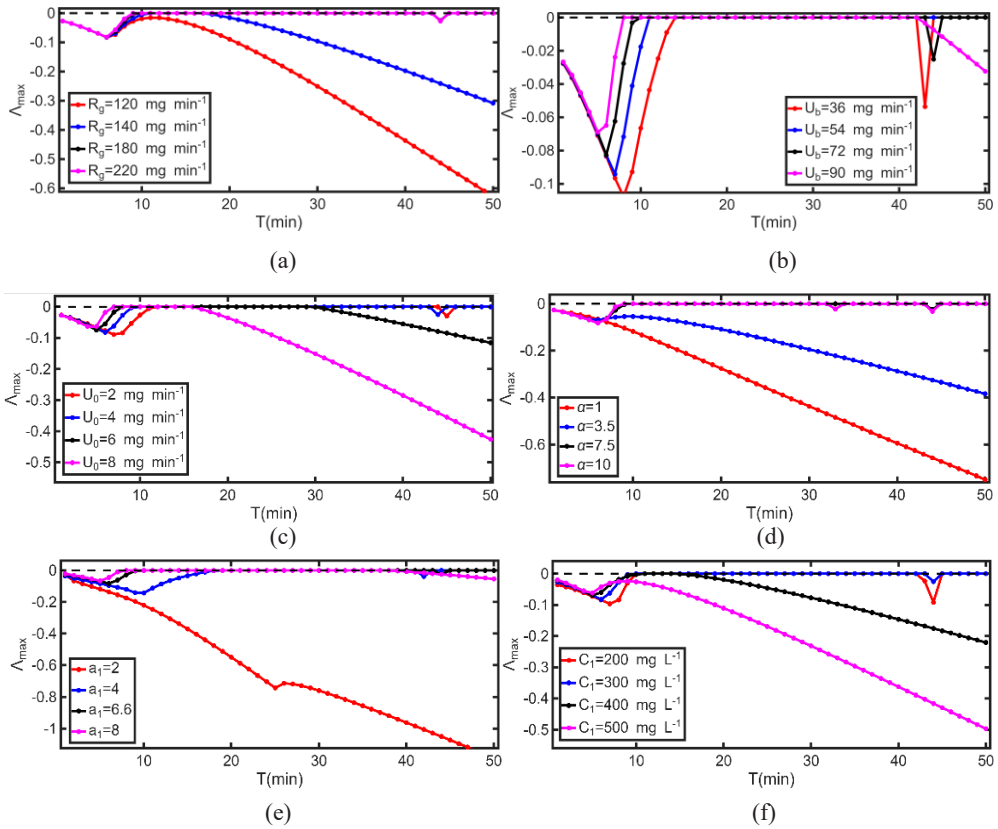

Fig. 7. The variation of MLE (Λ_{max}) with inter-kick time T induced by the U-K model (Eq. (1)) with T pulsatile forcing (Eq. (5)). The dotted line at $\Lambda_{max} = 0$ separates chaotic and non-chaotic regimes. The tuned parameter in each panel: (a) R_g, (b) U_b, (c) U_0, (d) α, (e) a_1 and (f) C_1. Kick amplitude: A = 10 mg/dL.

4.2 Fast Lyapunov Indicator (FLI)

The Fast Lyapunov Indicator (FLI) is a sensitive and efficient tool to detect chaotic behavior in nonlinear dynamical systems [18]. Since the maximal Lyapunov exponent (MLE) require long integration, highly sensitive measure of local instability, making it a powerful diagnostic tool for exploring the finite-time growth of deviation vectors and capturing the local instability of trajectories much more rapidly. The procedure of the integration scheme is exactly the same as earlier. The FLI is represented as

$$\mathrm{FLI} = \max_{0 \le k \le N} \ln\left(\frac{d_k}{d_0}\right),$$

where d_0 is the fixed initial separation, d_k is the separation after the k-th kick-relaxation cycle.

Fig. 8 shows a slow, nearly logarithmic increase in the FLI, which supports further this interpretation that the motion is quasi-periodic. In the forced oscillators, quasi-periodic

motion typically leads to this kind of sub-exponential divergence, unlike the rapid growth seen in chaotic systems.

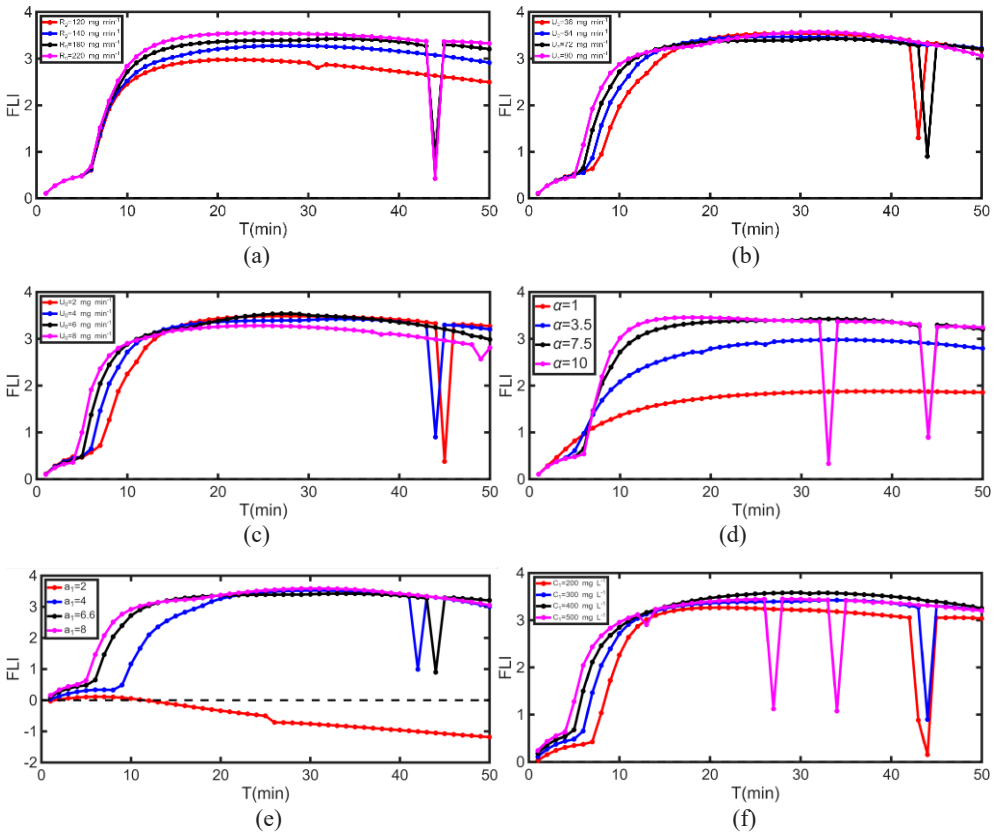

Fig. 8. The variation of FLI with inter-kick time T induced by the U-K model (Eq. (1)) with T pulsatile forcing (Eq. (5)). The tuned parameter in each panel: (a) R_g, (b) U_b, (c) U_0, (d) α, (e) a_1 and (f) C_1. Kick amplitude: A = 10 mg/dL.

5 Results and Discussions

From our simulations, we observe that the choice of numerical integrator has a clear impact on the computed Lyapunov indicators. While some solvers give consistent results, others tend to produce misleading values, especially when default tolerances are used.

In particular, stiff solvers sometimes give positive Lyapunov exponents even when the system is not truly chaotic. This occurs due to their larger time steps and smoothing behavior. As a result, they may distort the evolution of nearby trajectories. On the other hand, non-stiff solvers such as ode45 tend to capture the dynamics more accurately. They use smaller adaptive step sizes, which helps preserve the local structure of the trajectories. Thus, these positive values are not robust and disappear under tighter tolerances and consistent solver choices.

The earlier work proposed by Karamched *et al.*, used only MATLAB ode23s solver with default tolerances to calculate MLE that demonstrated chaotic behavior of this system [10, 11]. On the other hand, for our cases, we use four different MATLAB solvers (eg.

non-stiff solver (ode45, ode23) and stiff solver (ode15s, ode23s)), including default tolerances (relative tolerance-10^{-3}, absolute tolerance-10^{-6}) and tight tolerances (relative tolerance-10^{-9}, absolute tolerance-10^{-10}) to calculate MLE and compare our results with existing results. Except for the solution ode15s and ode23s, with default tolerances,

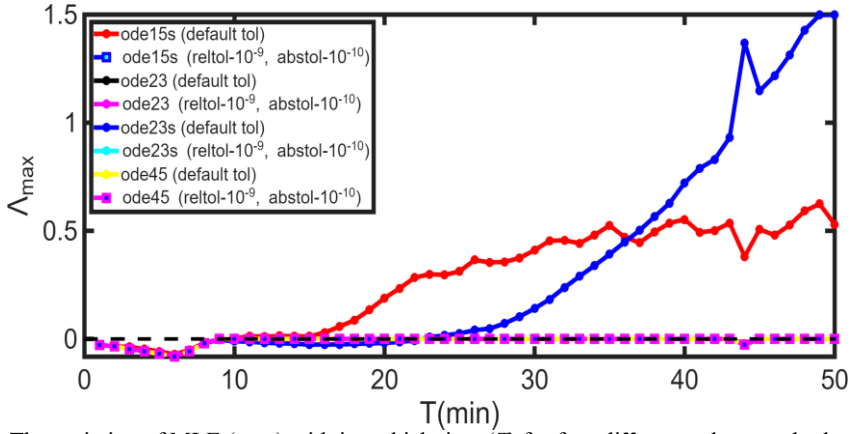

Fig. 9. The variation of MLE (Λ_{max}) with inter-kick time (T) for four different solvers and tolerances when R_g = 220 mg min^{-1}.

the MLE value does not show any positive value (Fig. 9). Since, most combinations of solvers and tolerances lead to similar results, i.e., the MLE values are negative or lie close to zero, it is clear that positive Lyapunov exponents are not reliable, as they vary with the choice of solver and tolerance.

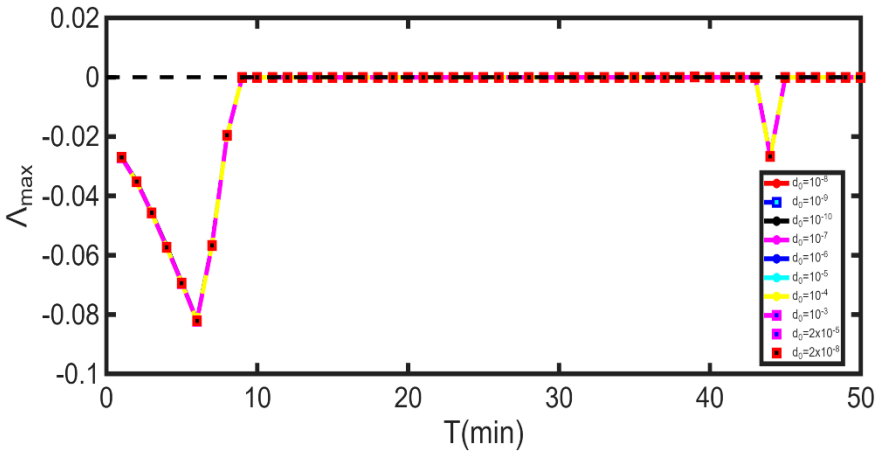

Fig. 10. The variation of MLE (Λ_{max}) with inter-kick time (T) for ten different initial conditions ns when R_g = 220 mg min^{-1}.

Furthermore, the maximal Lyapunov exponent (MLE) is evaluated over an ensemble of 10 initial conditions using MATLAB's ode45 integrator with default tolerances. As shown in Fig. 10, all exponents remain non-positive with negligible variation across different realizations. The observed non-positive result is consistent across different numerical integrators when appropriate solver settings and tolerances are carefully chosen. If the system were chaotic, the computed

Lyapunov exponents would show stronger sensitivity across different initial conditions. This consistency rules out chaotic dynamics and confirms that the observed behavior is robust and not an artifact of specific numerical methods. With accurate and consistent methods, the system shows behavior consistent with that of a periodically forced nonlinear oscillator, characterized by non-positive Lyapunov exponents and quasi-periodic phase space structure (Figs. 6–8). Together with the Lyapunov analysis, this indicates that the system does not exhibit intrinsic chaos. This indicates that earlier signs of chaos likely arise from numerical artifacts rather than from the system itself.

Conclusion

In this work, we have studied the glucose-insulin model using different numerical methods and chaos indicators. The previous study claimed in their study that this forced system can exhibit chaotic behavior due to delay [10, 11]. However, our results suggest that numerical choices can strongly influence the observed dynamics. We find that care must be taken while interpreting Lyapunov-based measures, as they can be affected by the integration scheme. In this sense, numerical validation becomes an important step in ensuring reliable results. Therefore, we conclude that this system does not exhibit any chaos rather the chaos depicted in previous work is a numerical artifact. In future work, it may be useful to explore data-driven approaches. These methods could help identify numerical artifacts and improve the robustness of the analysis.

References

1. P. S. Shabestari, K. Rajagopal, B. Safarbal, S. Jafari, P. Duraisamy, A Novel Approach to Numerical Modeling of Metabolic System: Investigation of Chaotic Behavior in Diabetes Mellitus. Complexity. **2018**, (2018). https://doi.org/10.1155/2018/6815190
2. B. Huard, A. Bridgewatera, M. Angelova, Mathematical investigation of diabetically impaired ultradian oscillations in the glucose-insulin regulation, J. Theor. Biol. **418**, 66-76 (2017). https://doi.org/10.1016/j.jtbi.2017.01.039
3. B. Huard, J. F. Easton, M. Angelova, Investigation of stability in a two-delay model of the ultradian oscillations in glucose–insulin regulation. Commun Nonlinear Sci Numer Simulat **26**, 1-3, 211–222 (2015). https://doi.org/10.1016/j.cnsns.2015.02.017
4. A. Drozdov, H. Khanina, A model for ultradian oscillations of insulin and glucose. Math. Comput. Model. **22**, 2, 23–38 (1995). https://doi.org/10.1016/0895-7177(95)00108-E
5. J. Sturis, K. Polonsky, E. Mosekilde, E. Van Cauter, Computer model for mechanisms underlying ultradian oscillations of insulin and glucose. Am. J. Physiol. **260**, 5, E801– E809 (1991). https://doi.org/10.1152/ajpendo.1991.260.5.E801
6. J. Li, Y. Kuang, C. Mason, Modeling the glucose-insulin regulatory system and ultradian insulin secretory oscillations with two explicit time delays. J. Theor. Biol. **242**, 3, 722–735 (2006). https://doi.org/10.1016/j.jtbi.2006.04.002
7. J. Keener, J. Sneyd, Mathematical physiology, interdisciplinary applied mathematics, vol. 8., (Springer-Verlag, New York xx+766, 1998).

8. J. Li, Y. Kuang, Analysis of a model of the glucose-insulin regulatory system with two delays. SIAM J. Appl. Math. **67**, 3, 757–776 (2007). https://doi.org/10.1137/050634001
9. A. A. Al-Hussein, F. Rahma, S. Jafari, Hopf bifurcation and chaos in time-delay model of glucose-insulin regulatory system. Chaos, Solitons & Fractals. **137**, 109845 (2020). https://doi.org/10.1016/j.chaos.2020.109845
10. B. Karamched, G. Hripcsak, D. Albers, W. Ott, Delay-induced uncertainty for a paradigmatic glucose–insulin model, Chaos. **31**, 2, (2021). https://doi.org/10.1063/5.0027682
11. B. R. Karamched, G. Hripcsak, R. L. Leibel, D. Albers and W. Ott, Delay-induced uncertainty in the glucose-insulin system: Pathogenicity for obesity and type-2 diabetes mellitus. Front. Physiol. **13**, (2022). https://doi.org/10.3389/fphys.2022.936101
12. D. J. Albers, M. E. Levine, L. Mamykina, G. Hripcsak, The parameter Houlihan: A solution to high-throughput identifiability indeterminacy for brutally ill-posed problems. Mathematical Biosciences. **316**, 108242 (2019). https://doi.org/10.1016/j.mbs.2019.108242
13. Q. Wang, L. S. Young, Strange Attractors in Periodically-Kicked Limit Cycles and Hopf Bifurcations. Commun. Math. Phys. **240**, 509–529 (2003). https://doi.org/10.1007/ s00220-003-0902-9
14. C. B. Moler, Numerical Computing with Matlab. (SIAM, Philadelphia, x + 330, 2008)
15. T. S. Parker, L.O. Chua, Practical Numerical Algorithms for Chaotic Systems, (Springer-Verlag, Heidelberg, XIV+348, 1989).
16. F. Diele, C. Marang, Geometric Numerical Integration in Ecological Modelling. Mathematics 2020. **8**, 1, (2019). https://doi.org/10.3390/math8010025
17. Skokos, Ch.: The Lyapunov Characteristic Exponents and Their Computation, Lect. Notes Phys. (Springer-Verlag, Heidelberg, **790**, 63–135, 2010).
18. C. Skokos, G. A. Gottwald, J. Laskar, Chaos Detection and Predictability, Lect. Notes Phys, vol. 915. (Springer-Verlag, Heidelberg, 2016).